Comparing Graphene Oxide and Reduced Graphene Oxide for DNA Adsorption and Sensing

Chang Lu[1, 2], Po-Jung Jimmy Huang[2], Biwu Liu[2], Yibin Ying[1,*] and Juewen Liu[2,*]

1. College of Biosystems Engineering and Food Science, Zhejiang University, Hangzhou 310058, China

Email: ybying@zju.edu.cn

2. Department of Chemistry, Waterloo Institute for Nanotechnology, University of Waterloo, Waterloo, Ontario, Canada, N2L 3G1.

Email: liujw@uwaterloo.ca

Abstract

Fluorescently labeled DNA adsorbed on graphene oxide (GO) is a well-established sensing platform for detecting a diverse range of analytes. GO is a loosely defined material and its oxygen content may vary depending on the condition of preparation. Sometimes, a further reduction step is intentionally performed to decrease the oxygen content and the resulting material is called reduced GO (rGO). In this work, DNA adsorption and desorption from GO and rGO is systematically compared. Under the same salt concentration, DNA adsorbs slightly faster with a 2.6-fold higher capacity on rGO. At the same time, adsorbed DNA on rGO is more resistant to desorption induced by temperature, pH, urea, and organic solvents. Various lengths and sequences of DNA probes have been tested. When its complementary DNA (cDNA) is added as a model target analyte, the rGO sample has a higher signal-to-background and signal-to-noise ratio, while the GO sample has a slightly higher absolute signal increase and faster signaling kinetics. Adsorbed DNAs on GO or rGO are still susceptible to non-specific displacement by other DNA and proteins. Overall, while rGO adsorb DNA more tightly, it allows efficient DNA sensing with an extremely low background signal.

Introduction

Graphene is a single layer of graphite with an extremely large specific surface area.[1, 2] To disperse in water, graphene oxide (GO) is often prepared by chemically exfoliating graphite under strong acidic and oxidative conditions, yielding hydroxyl, epoxy and carboxyl groups. Since its discovery, GO has been used for adsorbing many biomolecules, especially DNA.[3-5] For example, GO physisorbs DNA and it also quenches fluorescence. Adding a complementary DNA (cDNA) can desorb fluorescent probe DNA resulting in fluorescence enhancement.[6-11] In addition, amino-modified DNAs were covalently attached to the carboxyl groups on GO forming an amide bond, avoiding non-specific probe displacement.[12-15] Many DNA-related enzymes were also involved to introduce functions such as signal amplification.[16, 17] Finally, DNA/GO conjugates were used to template materials synthesis such as metal nanoparticles,[18-20] and stacked GO sheets.[21] Fundamental studies on the interaction between DNA and GO were also carried out.[11, 22-32]

GO is a loosely defined material, and the oxygen content can vary quite a lot depending on the preparation condition. The adsorption affinity of DNA is likely to depend on the oxygen content. A related material is called reduced GO (rGO), which is prepared by chemically reducing GO to decrease its oxygen content.[33] GO has poor electric conductivity due to its extensively disrupted π-conjugation system; while rGO has an intermediate conductivity and still retains the ability to disperse in water.

While most DNA-based sensing work used GO, interfacing DNA with rGO was also reported recently. For example, to develop DNA-based electrochemical sensors, rGO is more useful for its better electric conductivity.[34-36] Interestingly, the number of optical sensors using

rGO is quite limited,[36-39] despite that rGO is a better fluorescence quencher.[40] From the surface science perspective, rGO might adsorb DNA more tightly since it has a lower surface charge density (thus less electrostatic repulsion with negatively charged DNA). In addition, rGO has more aromatic regions for π-π stacking with DNA bases. Such tighter adsorption and stronger fluorescence quenching may decrease background.

By reading the literature, we found a diverse range of sensor performance with the same GO-based signaling method.[7, 13, 23, 25, 41] In addition to the difference in buffer composition, the difference in the oxidation level of GO might also contribute to such inconsistency. Therefore, a comprehensive fundamental understanding is critical to facilitate further rational sensor design. To this end, we compared DNA adsorption and desorption by GO and rGO, and related DNA sensing.

Materials and Methods

Chemicals. The DNA samples were from Integrated DNA Technologies (Coralville, IA). The DNA sequences used in this work are as follows: FAM-probe DNA: TTCTTCCT(FAM) CCTTGTT-NH_2; AF-A_{15}: AlexaFluor 647-AAAAAAAAAAAAAAA; T_{15}; FAM-T_{15}; FAM-A_{15}; FAM-T_{30}; A_{15}; A_{30}; T_{10}; T_{20}; T_{30}; cDNA: AACAAGGAGGAAGAA. All the sequences are listed from the 5′ to 3′-end. Carboxyl GO was purchased from ACS Material (Medford, MA). Sodium nitrate, sodium borohydride, sodium chloride, sodium hydroxide, sodium carbonate, sodium bicarbonate, magnesium chloride, 4-morpholineethanesulfonate (MES), tris(hydroxymethyl)aminomethane (Tris), and 4-(2-hydroxyethyl) piperazine-1-ethanesulfonate (HEPES) were from Mandel Scientific (Guelph, Ontario, Canada). Bovine serum albumin (BSA)

and N-(3-Dimethylaminopropyl)-N′-ethylcarbodiimide hydrochloride (EDC·HCl) were from Sigma- Aldrich. Milli-Q water was used for all the experiments.

Preparation of rGO and sensors. To prepare rGO, 150 μL of GO (0.33 mg/mL) was mixed with a final of 150 mM $NaBH_4$. After heating at 70 °C for 2 h, the sample was washed with water by centrifugation at 15,000 rpm for 10 min for three times. To absorb DNA, a solution of GO or rGO (0.33 mg/mL, 150 μL) was respectively incubated with FAM-labeled DNA (6.7 μM) in buffer A (25 mM HEPES, pH 7.5, 150 mM NaCl, 1 mM $MgCl_2$) in dark at room temperature for 1 h. Then the two sensors were washed with buffer A by centrifugation at 15,000 rpm for 10 min for six times. The physisorbed sensors were dispersed in buffer A and stored at 4 °C with a final GO and rGO concentration of 200 μg/mL (termed solution I and II, respectively).

XPS, UV-vis, and dynamic light scattering (DLS) spectroscopy. The XPS was performed on a Thermo-VG Scientific ESCALab 250 microprobe instrument with a monochromatic Al K-alpha source (1486.6 eV) using 0.33 mg GO or rGO. The electronic absorption of GO and rGO was measured on a UV-vis spectrometer (Agilent 8453A). The ζ-potential of GO and rGO (50 μg/mL) was measured by dynamic light scattering on a Malvern Zetasizer Nano ZS90 with a He-Ne laser (633 nm) at 90 degree collecting optics at 25 °C at various pH's in 10 mM buffer. The hydrodynamic size was measured using the same instrument in water.

DNA adsorption/desorption. The kinetics of DNA adsorption was studied by adding different concentrations of GO and rGO to 50 μL solution containing 0.4 μM FAM-probe DNA in buffer A at 25 °C. The fluorescence before adding GO was measured to be the initial intensity. Several different salt concentrations were also tested. Temperature-induced desorption of DNA was carried out in a real-time PCR thermocycler using a sample volume of 20 μL loaded in a 96-well

PCR plate containing 100 μg/mL of GO or rGO in 5 mM HEPES, pH 7.5. The temperature was increased every 1 °C with a holding time of 1 min before each reading. To study DNA desorption induced by chemicals, 5 μL solution I or II was centrifuged. After removing the supernatant, the pellet was dispersed in 50 μL of urea (4 or 8 M), NaOH (10 mM), or isopropanol solution. The fluorescence intensity of these samples was measured.

For cDNA-induced DNA desorption, each well contained 45 μL buffer A and 5 μL solution I or II. Then different concentrations of the cDNA was added to initiate the desorption reaction. Displacement of adsorbed DNA was studied by adding 0.4 μM of $T_{15}/A_{15}/T_{10}/T_{20}/T_{30}$ without fluorophore label or 0.1% BSA. For preparing the covalently linked sensor, the procedure was the same as previously reported.[15] Then the rGO with covalent DNA was prepared by further reducing using $NaBH_4$ as described above. Its signaling was measured after adding cDNA (final 4 μM).

Dual fluorophore DNA adsorption/desorption. The DNA/GO complex was prepared by mixing AF-A_{15} DNA (final 0.8 μM) with GO or rGO (100 μg/mL) in buffer A (final total volume 50 μL). FAM-labeled T_{15} (final concentration 2 μM) was then added to induce the desorption reaction. The desorption experiment was monitored with a fluorescence plate reader at two channels (Infinite F200 Pro, Tecan).

Results and Discussion

Experiment design overview. In this study, we aim to compare GO and rGO for their surface interaction with DNA. First, DNA adsorption was studied using fluorescently labeled oligonucleotides. Then we studied DNA desorption by adding its complementary DNA (cDNA),

non-cDNA and proteins, and by a few denaturing conditions including heat, base, urea, and isopropanol. The scheme of these reactions is shown in Figure 1. Since both GO and rGO are fluorescence quenchers, DNA adsorption is accompanied with fluorescence quenching and desorption is indicated by fluorescence enhancement.

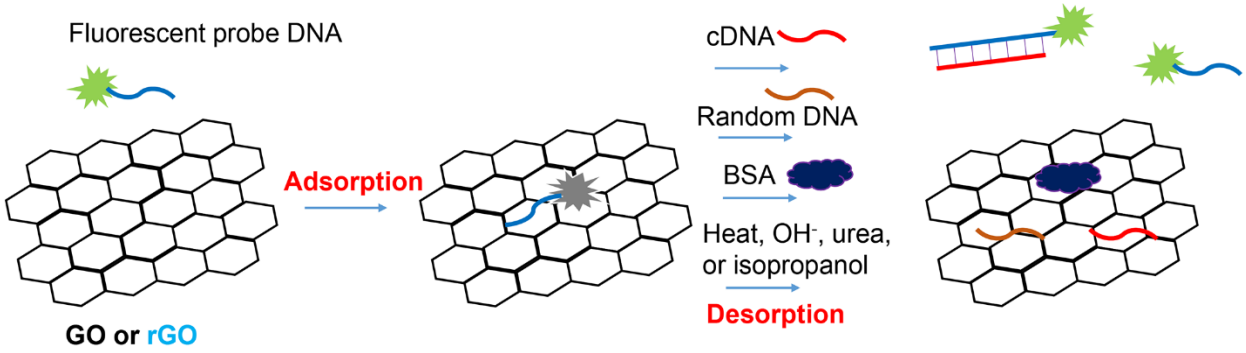

Figure 1. Schematics of a fluorescently-labeled DNA adsorbed by GO or rGO, resulting in fluorescence quenching. Under various conditions, the adsorbed DNA can be desorbed, resulting in fluorescence recovery. The goal is to compare GO and rGO for these reactions. The oxygen-containing groups and aromatic structures on GO or rGO are not drawn for clarity of the figure.

Characterization of GO and rGO. To compare GO and rGO, we first prepared rGO using GO as the starting material. For this purpose, GO was reduced using $NaBH_4$. The color of the sample turned from yellow for GO to black after the reduction (inset of Figure 2A). The electronic absorption was measured (Figure 2A) and an increase in the overall absorbance with a red shift is observed for the rGO, indicating a successful reduction reaction. The size of our GO and rGO sheets was determined to be ~900 nm using dynamic light scattering (DLS, Figure S1).

The GO and rGO samples were further characterized by X-ray photoelectron spectroscopy (XPS) to measure the oxygen content (Figure 2B, D). Our GO sample was rich in

carboxyl groups and also C-O single bonds. After reduction, the C-C bond became the major peak. The oxygen content decreased from 40.8% for GO to 18.8% after the reduction. Further reduction (e.g. with longer reaction time or higher $NaBH_4$ concentration) significantly decreased the colloidal stability of rGO in water, and the sample aggregated easily. Therefore, we employed the 18.8% oxygen rGO sample for the subsequent studies.

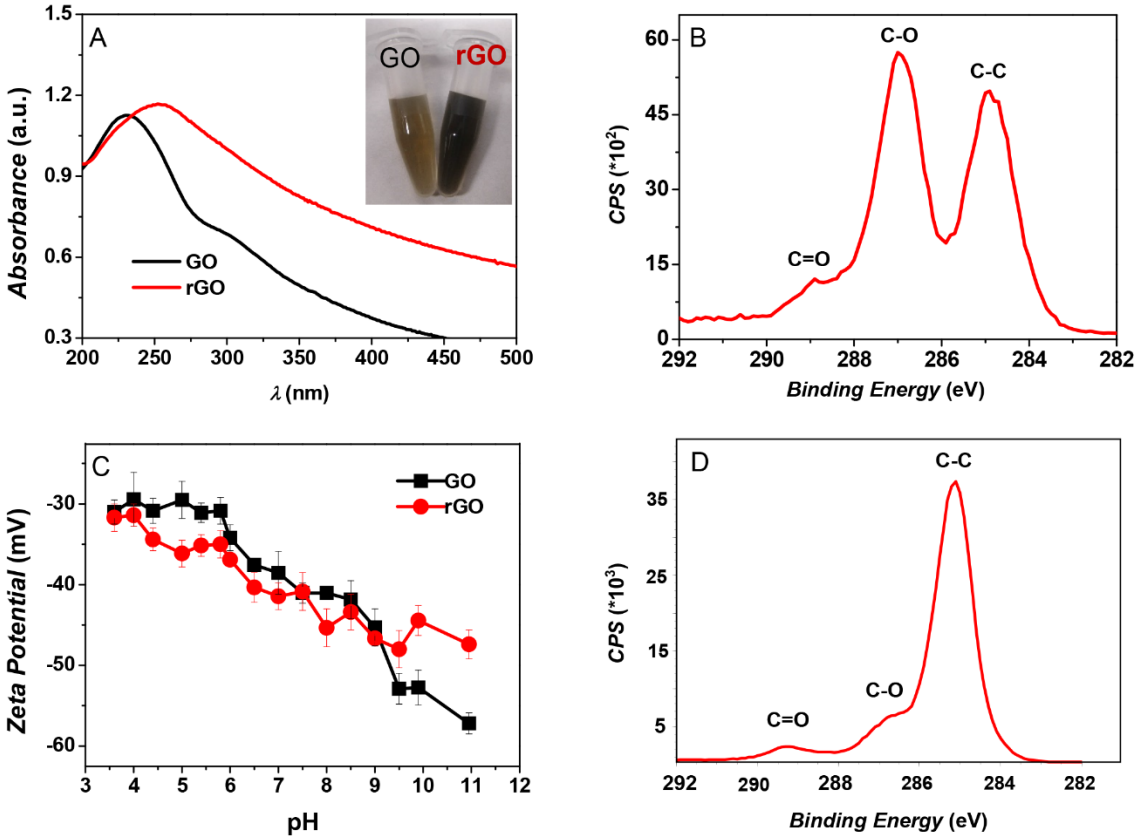

Figure 2. (A) Characterization of GO and rGO in water (0.1 mg/mL) by UV-vis spectrometry. Inset: a photograph of GO and rGO (0.2 mg/mL). The C1s XPS spectra of the (B) GO and (D) rGO. The peaks are assigned to the corresponding chemical species. (C) ζ-potential of GO and rGO from pH 3.6 to 11 in 10 mM buffer (acetate from pH 3.6 to 6; phosphate from pH 6 to 8.5; and carbonate from pH 9 to 11).

Since DNA is a polyanion, electrostatic interactions are likely to be important. We next measured the ζ-potential of both GO and rGO as a function of pH (Figure 2C). From pH 3.6 to 11, both samples are negatively charged. Under most conditions, especially near neutral pH, the ζ-potential of GO and rGO is very similar.[42] Therefore, even though rGO has a lower density of carboxyl groups, it still retains sufficient negative charges on the surface, which is important for its colloidal stability. The charges on a surface come from both ionization (e.g. carboxyl groups) and adsorption. The similar charge density on GO and rGO can be explained by the adsorption of more OH^- ions by the hydrophobic regions on rGO. It has been reported that hydrophobic surfaces selectively adsorb OH^- compared to H^+, leading to a negatively surface.[43]

rGO adsorbs more DNA and faster. Since DNA, GO and rGO are all negatively charged, salt concentration should be important for DNA adsorption. In a pH 7.5 buffer (10 mM HEPES), we mixed GO or rGO with a FAM-labeled DNA at five salt concentrations (Figure 3A, B). DNA adsorption was followed by fluorescence quenching. Without additional salt, DNA failed to adsorb on either GO or rGO due to strong electrostatic repulsion. With 100 mM NaCl, adsorption was observed as indicated by fluorescence quenching. With an additional 1 mM $MgCl_2$, adsorption was close to completion in just 1 min. In each case, the adsorption was more efficient on rGO. With 300 mM NaCl or 300 mM NaCl and 1 mM $MgCl_2$, adsorption was finished immediately after mixing for both GO and rGO. Overall, salt facilitates DNA adsorption. At the same buffer salt concentration, DNA adsorption by rGO is faster.

Next, we fixed the DNA and salt concentration, and varied the carbon concentration (Figure 3C, D). More fluorescence quenching occurred with more GO and rGO. At the same

concentration, fluorescence quenched more quickly with rGO. We plotted the relative fluorescence quenching at 10 min after mixing as a function of GO or rGO concentration, and this quenching reflects DNA adsorption capacity. Both samples followed a linear decaying trend initially (Figure 3E), and the slope of the rGO sample was 2.6-fold higher than that for the GO, suggesting that the rGO has 2.6-fold higher DNA adsorption capacity when DNA is in excess.

Note that our rGO samples were prepared by reducing and then extensive washing. It is likely that some rGO is lost in this work-up. At the same time, rGO tends to aggregate more easily than GO. While we assumed no loss in our concentration calculation, the actual surface area of rGO should be smaller than GO. However, rGO still has a higher DNA adsorption capacity, and faster DNA adsorption kinetics. This indicates that DNA is adsorbed more favorably on the carbon-rich domains than on the oxygen-rich GO. The reason for the enhanced DNA adsorption by rGO is attributable to the more carbon-rich surface allowing better π-π stacking with the DNA bases, which is a main force for DNA adsorption.[31, 44]

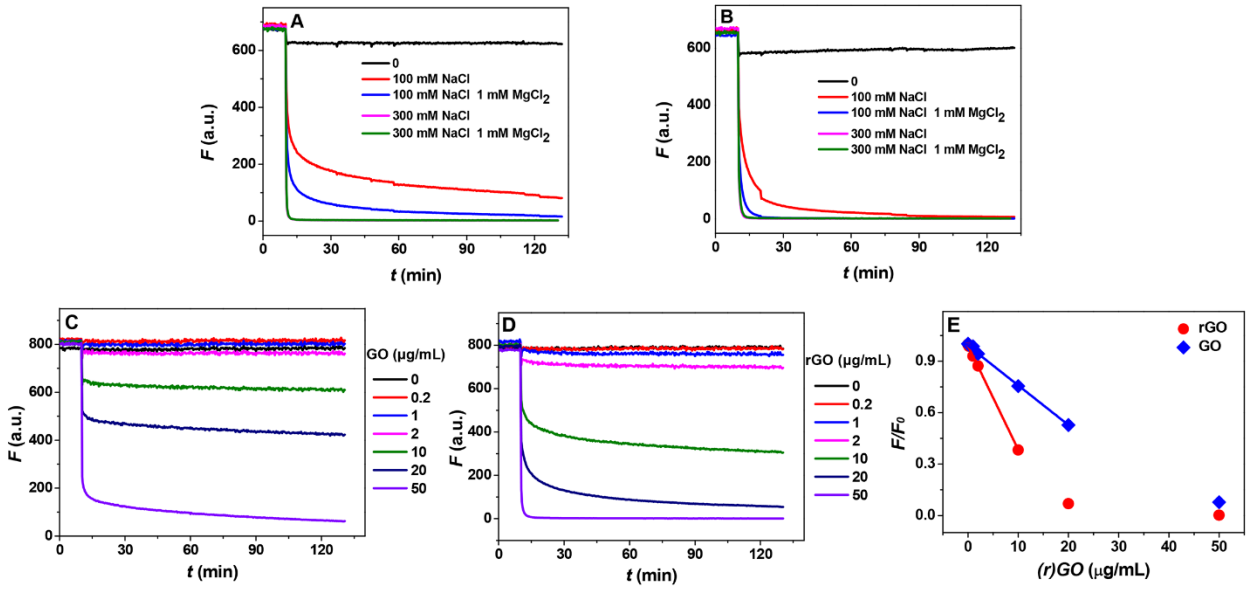

Figure 3. A comparison of GO and rGO for DNA adsorption. Adsorption kinetics of 0.4 μM FAM-labeled DNA on (A) GO and (B) rGO (50 μg/mL each) in buffer (10 mM HEPES, pH 7.5) with different salt concentrations. (C) DNA adsorption kinetics by various concentrations of (C) GO and (D) rGO in buffer A (10 mM HEPES, pH 7.5 with 150 mM NaCl and 1 mM $MgCl_2$). GO or rGO was added at 10 min for all the experiments. (E) Relative fluorescence quenching by various concentrations of GO and rGO at 20 min. *F* presents fluorescence at 20 min and F_0 means the initial fluorescence.

DNA adsorbed on rGO more strongly probed by denaturing conditions. After understanding DNA adsorption, we next studied desorption. DNA desorption can be induced by a number of denaturing conditions, such as high temperature, urea, base, and organic solvents. These factors were studied one at a time. We first studied the effect of temperature. The FAM-labeled DNA was adsorbed on GO and rGO, respectively, and their fluorescence was monitored with gradually increased temperature (Figure 4A). This is similar to measuring the melting curve of DNA. The DNA on GO has a slightly higher background, but a large fluorescence increase is observed upon heating, indicating efficient DNA desorption. This sample has a broad melting profile, spanning from 30 °C to over 90 °C. Therefore, DNA is adsorbed with a diverse range of affinities on GO, which is consistent with its highly heterogeneous surface structure.[45] On the other hand, the amount of fluorescence increase is much smaller for the rGO and only a very small fluorescence increase occurs above 50 °C. This indicates a tighter adsorption affinity on rGO, and most DNA cannot be desorbed by thermal denaturation. The first derivatives of these melting curves are shown in Figure 4B. A meting transition centered at ~60 °C is observed with GO, while the rGO sample has no well-defined melting transitions.

Next, we added urea to the adsorbed DNA samples to probe hydrogen bonding (Figure 4C). A high concentration of urea can disrupt hydrogen bonds. With 4 M or 8 M urea, DNA desorbed from GO was at least 3 times of that from rGO. This suggests that hydrogen bonding is a more important force for DNA adsorption by GO,[26] and it also reflects the overall lower DNA adsorption stability by GO.

Raising pH can increase the negative charge density on the graphene samples, which should increase the electrostatic repulsion with DNA and thus induce DNA desorption. After adding 10 mM NaOH, we monitored the fluorescence increase. Again, the GO released more DNA than rGO did (Figure 4D). We also compared the stability of the adsorbed complexes in different salt concentrations. For this purpose, we dispersed the pre-adsorbed complexes with final NaCl concentrations from 15 to 300 mM (Figure S3). With 300 mM NaCl, both GO and rGO stably adsorbed the DNA, while at lower NaCl concentrations, desorption was observed on both surfaces with more desorption occurred on GO.

Finally, the effect of an organic solvent (isopropanol) was used to probe hydrophobic interactions (Figure 4E). The overall desorption was quite low from both GO and rGO. Again, at each tested isopropanol concentration, DNA desorbed more from GO. It is believed that DNA base stacking with the carbon-rich regions on GO or rGO is an important force for DNA adsorption.[27, 46, 47] Despite this, DNA is still adsorbed more stably on the rGO in this organic solvent. Therefore, under all tested conditions, DNA is more stably desorbed from GO than from rGO.

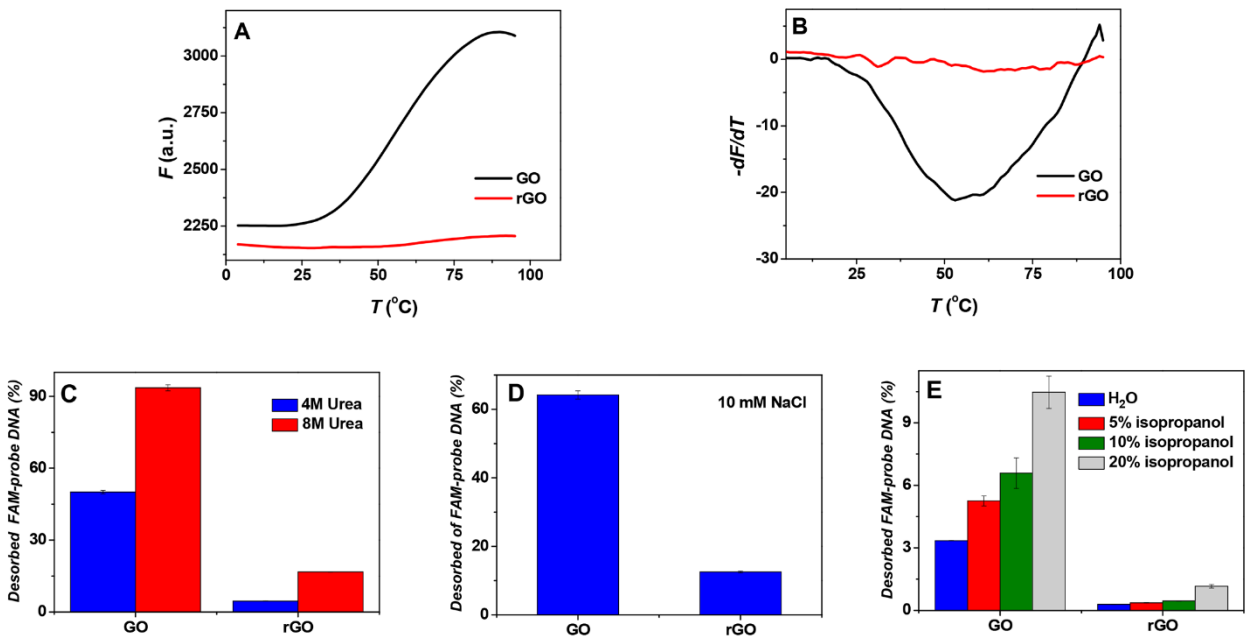

Figure 4. A comparison of DNA desorption from GO and rGO under various denaturing conditions. (A) Thermal desorption of the FAM-probe DNA from 100 μg/mL GO or rGO in buffer (5 mM HEPES, pH 7.5). (B) The first derivative of the data in (A). Fluorescence measurement of DNA desorption from GO and rGO after 5 min reaction with (C) 4 M or 8 M urea, (D) 10 mM NaOH, and (E) various concentrations of isopropanol. No salt was used for the experiments to facilitate DNA desorption.

DNA desorption by cDNA. Most work on DNA or RNA detection using GO relies on cDNA-induced probe desorption.[48-50] Considering its analytical importance, we next compared the detection of cDNA using the FAM-labeled DNA adsorbed by GO and rGO. The GO sample had a high background of about 30 fluorescence unit (Figure 5A). With the addition of cDNA, a gradual fluorescence increase was observed and more cDNA produced higher fluorescence

signal, consistent with previous observations. The rGO sample had a similar overall trend but with a much lower background fluorescence.

Two kinetic phases are identified for each sample.[25] Initially the DNA release was very fast, followed by a slower phase. It is likely that some weakly adsorbed DNA are more efficiently desorbed followed by the more strongly adsorbed DNA. The GO sample has more weakly adsorbed DNA (e.g. more fluorescence increase in the first kinetic phase), while the rGO sample has more strongly adsorbed DNA (e.g. more fluorescence increase in the second kinetic phase). Finally, if the absolute fluorescence increase is compared, the rGO sample is just slightly lower by ~15% (Figure 5C).

In both samples, a higher concentration of cDNA induced stronger final fluorescence signal, allowing quantitative DNA detection. To have a better comparison, we plotted their signal-to-background ratio (Figure 5D) and signal-to-noise ratio (Figure 5E), which are related to the sensitivity of the sensors. The signal-to-background ratio was up to 4-fold higher for the rGO sample, mainly due to its very low background. The signal-to-noise ratio is also higher for the rGO (by up to 2-fold). The presence of a large amount of free probe DNA in the GO sample is likely to be the reason for its higher background variation. Therefore, rGO has a better sensing performance.

The above measurements were performed with only one probe DNA sequence. To test the generality of our observation, a few more FAM-labeled probes were used, including both poly-A and poly-T 15-mer homopolymers, and also poly-T DNA of different lengths (Figure S3-S5). We did not test poly-C or poly-G DNA since they tend to form various secondary structures and will complicate data interpretation. In each case, the rGO sample has a higher signal-to-background ratio. We further studied the effect of the concentration of GO and rGO with fixed

0.4 μM FAM-T15 probe (Figure S6). In both cases (20 and 50 μg/mL), the rGO still showed better signal increase due to its lower background signal. For the same materials, a high concentration of GO or rGO absorbs DNA better, leading to lower background.

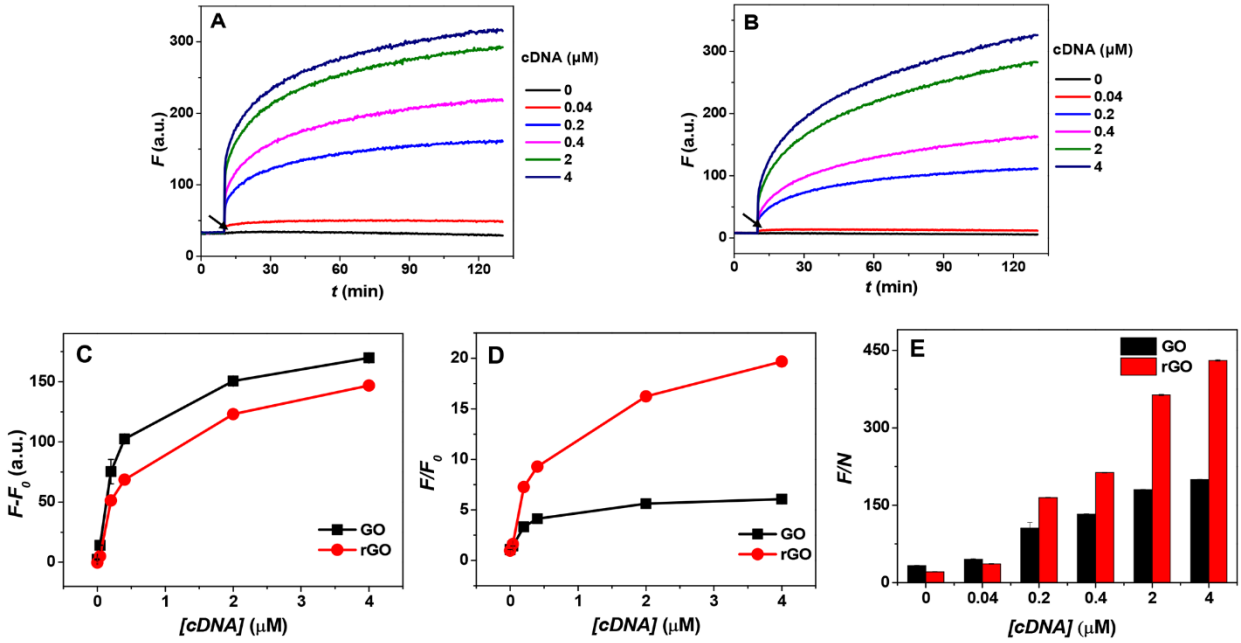

Figure 5. A comparison of cDNA-induced probe DNA desorption from GO and rGO. Desorption kinetics of the FAM-probe DNA from (A) GO and (B) rGO in the presence of various concentrations of cDNA. The arrows indicate the time point when cDNA was added (10min). The (C) absolute unit of fluorescence increase after 10 min reaction, (D) relative fluorescence enhancements or signal-to-background ratio, and (E) signal-to-noise ratio comparison for the GO and rGO samples. F_0 is the background fluorescence, F is the fluorescence after 10 min reaction, and N is the variation of the background signal in the absence of cDNA.

Non-specific displacement. Since the DNA probe was only physisorbed in all the above studies, in additional to cDNA, other molecules may also non-specifically displace the probe and thus

result in a false positive signal. Ideal sensors should only respond to the intended target analytes. To also compare this aspect, we next studied their resistance to non-specific displacement. For this experiment, FAM-labeled T_{15} was used as a probe. We tested DNA displacement by adding non-labeled A_{15}/T_{15}/T_{10}/T_{20}/T_{30} DNA (Figure 6A, 6B). In this case, the rGO sample appeared to be more resistant to non-specific DNA displacement. We further added bovine serum albumin (BSA, Figure 6C). In this case, both GO and rGO showed a similar absolute fluorescence enhancement, indicating that a similar number of probe DNA molecules was desorbed. Therefore, while rGO has a higher affinity for adsorbing the probe DNA, it also has a higher affinity with the proteins, leading to an overall similar response regardless of the oxidation level. Overall, the the rGO sample is better at resisting non-specific DNA than proteins.

Covalent linking the probe DNA to GO is a useful method to minimize non-specific probe desorption.[13-15] Therefore, we also compared the covalent sensors by using an amino and FAM dual labeled DNA (Figure 6D). Since reducing GO significantly decreased the number of carboxyl groups needed for covalent DNA conjugation, we prepared the rGO sample by first performing the DNA conjugation reaction followed by the reducing reaction. After adding cDNA, the signal of GO increased more than rGO, suggesting that reducing procedure did not increase the response of the covalent sensor.

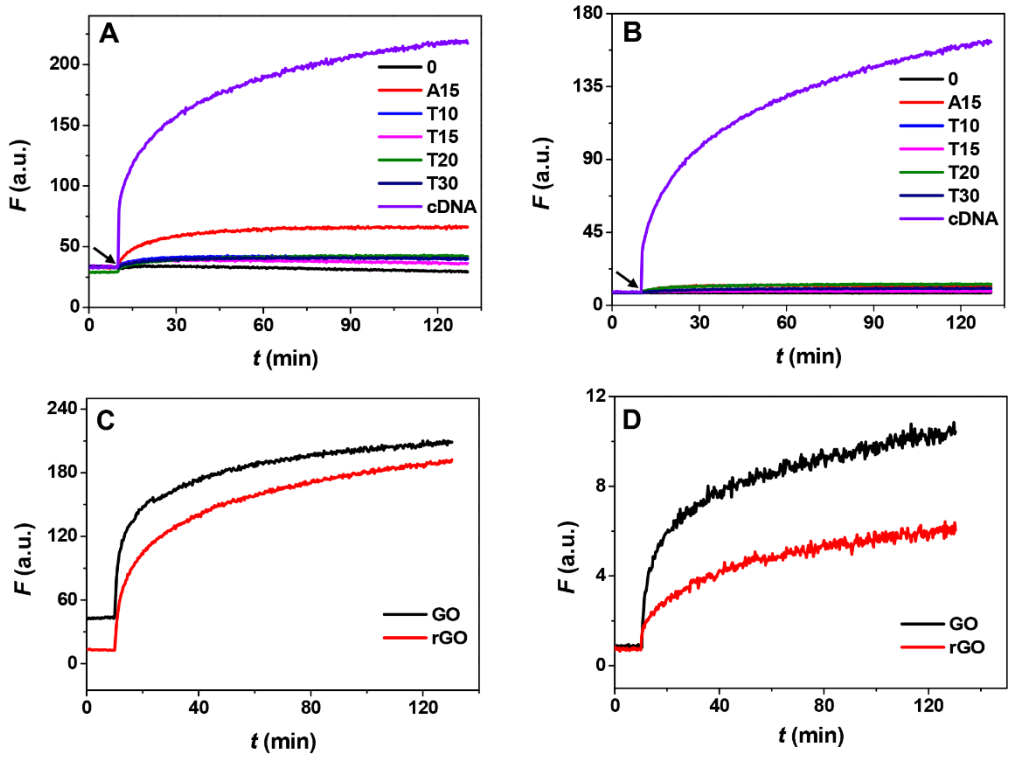

Figure 6. Probe (FAM-T_{15}) desorption induced by the cDNA and by non-specific displacement with 0.4 μM A_{15}/T_{15}/T_{10}/T_{20}/T_{30} but without the FAM label for (A) GO and (B) rGO. (C) Probe displacement by 0.1% BSA (buffer: 25 mM HEPES, 150 mM $NaNO_3$). (D) Kinetics of signaling by adding the cDNA (4 μM) in buffer A with 20 μg/mL covalently attached FAM-probe DNA on GO and rGO.

Quantitative surface mechanism studies using dual probes. In the ideal case, each cDNA should hybridize with an adsorbed probe to produce a fluorescence signal. However, this is not the case for GO-based sensors. If the probe density is low, it can take six cDNAs to produce one hybridization event, and the rest cDNA was used for non-specifically displacing the target DNA into solution.[24] To quantitatively compare this reaction on GO and rGO, we respectively adsorbed AlexaFluor 647 (AF)-labeled A_{15} DNA on these two surfaces. Then, FAM-labeled T_{15}

was added, and the increase of the AF emission was monitored at the same time with the decrease of the FAM emission (Figure 7A).

Similar to our previous results, more signal was produced from GO (Figure 7B, blue trace on top), indicating more probe DNA desorption. At the same time, more cDNA was adsorbed by GO (Figure 7C, blue trace at the bottom). For GO, during the time course of this reaction, ~0.082 μM probe desorbed and ~0.164 μM of the cDNA adsorbed. Therefore, each 2 cDNA molecules produced one probe signal. This is more efficient than what we previously reported (6 cDNA for 1 probe signal) because here the probe DNA was adsorbed at a higher density. For rGO, ~0.045 μM probe DNA desorbed and ~0.104 μM cDNA was adsorbed, corresponding to each 2.3 cDNAs producing one signal. Therefore, the efficiency of using the cDNA (i.e. the target DNA) is quite similar, and GO was just slightly more efficient. This is also consistent with the stronger signal intensity produced by GO. This can be attributed to the tighter adsorption of the probe DNA by rGO than by GO.

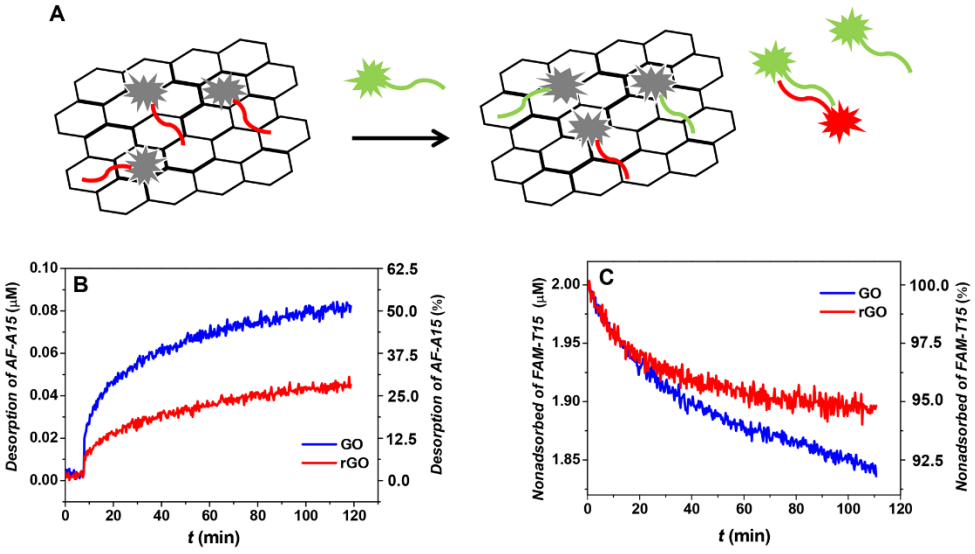

Figure 7. (A) A scheme of dual probes studying the efficiency of DNA hybridization on GO and rGO. (B) Desorption of AF-A_{15} by FAM-T_{15} DNA. (C) Adsorption of FAM-labeled DNA in the

presence of pre-adsorbed AF-A_{15}. The plots were made to compare both the percentage (the right axis) and absolute concentration (the left axis) of DNA adsorption/desorption.

Conclusions

In conclusion, we compared DNA adsorption and desorption from GO and rGO, and in particular, the implication for DNA sensing. A key conclusion is that DNA is adsorbed more tightly by rGO as probed by various denaturing conditions, leading to a higher adsorption capacity, faster adsorption kinetics, and lower background fluorescence signal. The rGO adsorbed DNA more tightly since it has lower surface negative charge and more aromatic regions for π-π stacking with DNA bases. Despite the tighter adsorption, cDNA-induced probe desorption still takes place efficiently on rGO, although the signaling kinetics is slightly slower and the absolute number of desorbed DNA is ~15% less compare to that from GO. However, both GO and rGO are similarly susceptible to non-specific displacement by biopolymers such as proteins. These basic understandings of the surface interaction between DNA and GO or rGO are valuable for design and optimization of sensors and devices based on these molecules and materials. Overall, rGO is an excellent platform for designing DNA-based biosensors.

Acknowledgement

This work is supported by the Natural Sciences and Engineering Research Council of Canada (NSERC). Chang Lu is supported by a Doctoral Fund for Priority Development Project from the Ministry of Education of China (20120101130009).

Supporting Information Available

This information is available free of charge via the Internet at http://pubs.acs.org/.

DSC spectra and additional DNA desorption kinetics as a function of DNA length and sequence (PDF).

References

(1) Geim, A. K.; Novoselov, K. S., The Rise of Graphene. *Nat. Mater.* **2007**, 6, 183-191.

(2) Novoselov, K. S.; Falko, V. I.; Colombo, L.; Gellert, P. R.; Schwab, M. G.; Kim, K., A Roadmap for Graphene. *Nature* **2012**, 490, 192-200.

(3) Loh, K. P.; Bao, Q.; Eda, G.; Chhowalla, M., Graphene Oxide as a Chemically Tunable Platform for Optical Applications. *Nat Chem* **2010**, 2, 1015-1024.

(4) Chen, D.; Feng, H.; Li, J., Graphene Oxide: Preparation, Functionalization, and Electrochemical Applications. *Chem. Rev.* **2012**, 112, 6027-6053.

(5) Yang, K.; Feng, L.; Shi, X.; Liu, Z., Nano-Graphene in Biomedicine: Theranostic Applications. *Chem. Soc. Rev.* **2013**, 42, 530-547.

(6) Wang, H.; Yang, R. H.; Yang, L.; Tan, W. H., Nucleic Acid Conjugated Nanomaterials for Enhanced Molecular Recognition. *ACS Nano* **2009**, 3, 2451-2460.

(7) Lu, C. H.; Yang, H. H.; Zhu, C. L.; Chen, X.; Chen, G. N., A Graphene Platform for Sensing Biomolecules. *Angew. Chem. Int. Ed.* **2009**, 48, 4785-4787.

(8) Liu, Z.; Liu, B.; Ding, J.; Liu, J., Fluorescent Sensors Using DNA-Functionalized Graphene Oxide. *Anal. Bioanal. Chem.* **2014**, 406, 6885-6902.

(9) He, S. J.; Song, B.; Li, D.; Zhu, C. F.; Qi, W. P.; Wen, Y. Q.; Wang, L. H.; Song, S. P.; Fang, H. P.; Fan, C. H., A Graphene Nanoprobe for Rapid, Sensitive, and Multicolor Fluorescent DNA Analysis. *Adv. Funct. Mater.* **2010**, 20, 453-459.

(10) Chang, H. X.; Tang, L. H.; Wang, Y.; Jiang, J. H.; Li, J. H., Graphene Fluorescence Resonance Energy Transfer Aptasensor for the Thrombin Detection. *Anal. Chem.* **2010**, 82, 2341-2346.

(11) Zhao, X. H.; Kong, R. M.; Zhang, X. B.; Meng, H. M.; Liu, W. N.; Tan, W. H.; Shen, G. L.; Yu, R. Q., Graphene-DNAzyme Based Biosensor for Amplified Fluorescence "Turn-on" Detection of Pb^{2+} with a High Selectivity. *Anal. Chem.* **2011**, 83, 5062-5066.

(12) Mohanty, N.; Berry, V., Graphene-Based Single-Bacterium Resolution Biodevice and DNA Transistor: Interfacing Graphene Derivatives with Nanoscale and Microscale Biocomponents. *Nano Lett.* **2008**, 8, 4469-4476.

(13) Huang, P.-J. J.; Liu, J., A Molecular Beacon Lighting up on Graphene Oxide. *Anal. Chem.* **2012**, 84, 4192-4198.

(14) Liu, Z.; Chen, S.; Liu, B.; Wu, J.; Zhou, Y.; He, L.; Ding, J.; Liu, J., Intracellular Detection of ATP Using an Aptamer Beacon Covalently Linked to Graphene Oxide Resisting Nonspecific Probe Displacement. *Anal. Chem.* **2014**, 86, 12229-12235.

(15) Lu, C.; Jimmy Huang, P.-J.; Ying, Y.; Liu, J., Covalent Linking DNA to Graphene Oxide and Its Comparison with Physisorbed Probes for Hg^{2+} Detection. *Biosens. Bioelectron.* **2016**, 79, 244-250.

(16) Jang, H.; Kim, Y. K.; Kwon, H. M.; Yeo, W. S.; Kim, D. E.; Min, D. H., A Graphene-Based Platform for the Assay by Helicase. *Angew. Chem. Int. Ed.* **2010**, 49, 5703-5707.

(17) Lu, C.-H.; Li, J.; Lin, M.-H.; Wang, Y.-W.; Yang, H.-H.; Chen, X.; Chen, G.-N., Amplified Aptamer-Based Assay through Catalytic Recycling of the Analyte. *Angew. Chem., Int. Ed.* **2010**, 49, 8454-8457.

(18) Liu, J.; Li, Y.; Li, Y.; Li, J.; Deng, Z., Noncovalent DNA Decorations of Graphene Oxide and Reduced Graphene Oxide toward Water-Soluble Metal-Carbon Hybrid Nanostructures via Self-Assembly. *J. Mater. Chem.* **2010**, 20, 900-906.

(19) Ocsoy, I.; Gulbakan, B.; Chen, T.; Zhu, G.; Chen, Z.; Sari, M. M.; Peng, L.; Xiong, X.; Fang, X.; Tan, W., DNA-Guided Metal-Nanoparticle Formation on Graphene Oxide Surface. *Adv. Mater.* **2013**, 25, 2319–2325.

(20) Ocsoy, I.; Paret, M. L.; Ocsoy, M. A.; Kunwar, S.; Chen, T.; You, M.; Tan, W., Nanotechnology in Plant Disease Management: DNA-Directed Silver Nanoparticles on Graphene Oxide as an Antibacterial against Xanthomonas Perforans. *ACS Nano* **2013**, 7, 8972-8980.

(21) Tang, L. H.; Wang, Y.; Liu, Y.; Li, J. H., DNA-Directed Self-Assembly of Graphene Oxide with Applications to Ultrasensitive Oligonucleotide Assay. *ACS Nano* **2011**, 5, 3817-3822.

(22) Tang, Z. W.; Wu, H.; Cort, J. R.; Buchko, G. W.; Zhang, Y. Y.; Shao, Y. Y.; Aksay, I. A.; Liu, J.; Lin, Y. H., Constraint of DNA on Functionalized Graphene Improves Its Biostability and Specificity. *Small* **2010**, 6, 1205-1209.

(23) Wu, M.; Kempaiah, R.; Huang, P.-J. J.; Maheshwari, V.; Liu, J., Adsorption and Desorption of DNA on Graphene Oxide Studied by Fluorescently Labeled Oligonucleotides. *Langmuir* **2011**, 27, 2731–2738.

(24) Liu, B.; Sun, Z.; Zhang, X.; Liu, J., Mechanisms of DNA Sensing on Graphene Oxide. *Anal. Chem.* **2013**, 85, 7987-7993.

(25) Park, J. S.; Goo, N.-I.; Kim, D.-E., Mechanism of DNA Adsorption and Desorption on Graphene Oxide. *Langmuir* **2014**, 30, 12587-12595.

(26) Park, J. S.; Na, H.-K.; Min, D.-H.; Kim, D.-E., Desorption of Single-Stranded Nucleic Acids from Graphene Oxide by Disruption of Hydrogen Bonding. *Analyst* **2013**, 138, 1745-1749.

(27) Varghese, N.; Mogera, U.; Govindaraj, A.; Das, A.; Maiti, P. K.; Sood, A. K.; Rao, C. N. R., Binding of DNA Nucleobases and Nucleosides with Graphene. *ChemPhysChem* **2009**, 10, 206-210.

(28) Manohar, S.; Mantz, A. R.; Bancroft, K. E.; Hui, C.-Y.; Jagota, A.; Vezenov, D. V., Peeling Single-Stranded DNA from Graphite Surface to Determine Oligonucleotide Binding Energy by Force Spectroscopy. *Nano Lett.* **2008**, 8, 4365-4372.

(29) Iliafar, S.; Mittal, J.; Vezenov, D.; Jagota, A., Interaction of Single-Stranded DNA with Curved Carbon Nanotube Is Much Stronger Than with Flat Graphite. *J. Am. Chem. Soc.* **2014**, 136, 12947-12957.

(30) He, Y.; Jiao, B.; Tang, H., Interaction of Single-Stranded DNA with Graphene Oxide: Fluorescence Study and Its Application for S1 Nuclease Detection. *RSC Adv.* **2014**, 4, 18294-18300.

(31) Lee, J.; Yim, Y.; Kim, S.; Choi, M.-H.; Choi, B.-S.; Lee, Y.; Min, D.-H., In-Depth Investigation of the Interaction between DNA and Nano-Sized Graphene Oxide. *Carbon* **2016**, 97, 92-98.

(32) Liu, B.; Huang, P.-J. J.; Kelly, E. Y.; Liu, J., Graphene Oxide Surface Blocking Agents Can Increase the DNA Biosensor Sensitivity. *Biotechnol. J.* **2016**, 11, 780-787.

(33) Erickson, K.; Erni, R.; Lee, Z.; Alem, N.; Gannett, W.; Zettl, A., Determination of the Local Chemical Structure of Graphene Oxide and Reduced Graphene Oxide. *Adv. Mater.* **2010**, 22, 4467-4472.

(34) Zhou, M.; Zhai, Y. M.; Dong, S. J., Electrochemical Sensing and Biosensing Platform Based on Chemically Reduced Graphene Oxide. *Anal. Chem.* **2009**, 81, 5603-5613.

(35) Yin, Z.; He, Q.; Huang, X.; Zhang, J.; Wu, S.; Chen, P.; Lu, G.; Zhang, Q.; Yan, Q.; Zhang, H., Real-Time DNA Detection Using Pt Nanoparticle-Decorated Reduced Graphene Oxide Field-Effect Transistors. *Nanoscale* **2012**, 4, 293-297.

(36) Liu, M.; Song, J.; Shuang, S.; Dong, C.; Brennan, J. D.; Li, Y., A Graphene-Based Biosensing Platform Based on the Release of DNA Probes and Rolling Circle Amplification. *ACS Nano* **2014**, 8, 5564-5573.

(37) Zhang, Y.; Zhao, H.; Wu, Z.; Xue, Y.; Zhang, X.; He, Y.; Li, X.; Yuan, Z., A Novel Graphene-DNA Biosensor for Selective Detection of Mercury Ions. *Biosens. Bioelectron.* **2013**, 48, 180-187.

(38) Abdelhamid, H. N.; Wu, H.-F., Reduced Graphene Oxide Conjugate Thymine as a New Probe for Ultrasensitive and Selective Fluorometric Determination of Mercury(II) Ions. *Microchimica Acta* **2015**, 182, 1609-1617.

(39) Kim, M.-G.; Shon, Y.; Lee, J.; Byun, Y.; Choi, B.-S.; Kim, Y. B.; Oh, Y.-K., Double Stranded Aptamer-Anchored Reduced Graphene Oxide as Target-Specific Nano Detector. *Biomaterials* **2014**, 35, 2999-3004.

(40) Kim, J.; Cote, L. J.; Kim, F.; Huang, J., Visualizing Graphene Based Sheets by Fluorescence Quenching Microscopy. *J. Am. Chem. Soc.* **2010**, 132, 260-267.

(41) He, S.; Song, B.; Li, D.; Zhu, C.; Qi, W.; Wen, Y.; Wang, L.; Song, S.; Fang, H.; Fan, C., A Graphene Nanoprobe for Rapid, Sensitive, and Multicolor Fluorescent DNA Analysis. *Adv. Func. Mater.* **2010**, 20, 453-459.

(42) Cote, L. J.; Kim, J.; Zhang, Z.; Sun, C.; Huang, J. X., Tunable Assembly of Graphene Oxide Surfactant Sheets: Wrinkles, Overlaps and Impacts on Thin Film Properties. *Soft Matter* **2010**, 6, 6096-6101.

(43) Tian, C. S.; Shen, Y. R., Structure and Charging of Hydrophobic Material/Water Interfaces Studied by Phase-Sensitive Sum-Frequency Vibrational Spectroscopy. *Proc. Natl. Acad. Sci. U.S.A.* **2009**, 106, 15148-15153.

(44) Liu, J., Adsorption of DNA onto Gold Nanoparticles and Graphene Oxide: Surface Science and Applications. *Phys. Chem. Chem. Phys.* **2012**, 14, 10485-10496.

(45) Gomez-Navarro, C.; Meyer, J. C.; Sundaram, R. S.; Chuvilin, A.; Kurasch, S.; Burghard, M.; Kern, K.; Kaiser, U., Atomic Structure of Reduced Graphene Oxide. *Nano Lett.* **2010**, 10, 1144-1148.

(46) Antony, J.; Grimme, S., Structures and Interaction Energies of Stacked Graphene-Nucleobase Complexes. *Phys. Chem. Chem. Phys.* **2008**, 10, 2722-2729.

(47) Gowtham, S.; Scheicher, R. H.; Ahuja, R.; Pandey, R.; Karna, S. P., Physisorption of Nucleobases on Graphene: Density-Functional Calculations. *Phys. Rev. B* **2007**, 76, 033401.

(48) Lu, Z.; Zhang, L.; Deng, Y.; Li, S.; He, N., Graphene Oxide for Rapid MicroRNA Detection. *Nanoscale* **2012**, 4, 5840-5842.

(49) Hizir, M. S.; Balcioglu, M.; Rana, M.; Robertson, N. M.; Yigit, M. V., Simultaneous Detection of Circulating Oncomirs from Body Fluids for Prostate Cancer Staging Using Nanographene Oxide. *ACS Appl. Mater. Interfaces* **2014**, 6, 14772-14778.

(50) Robertson, N. M.; Salih Hizir, M.; Balcioglu, M.; Wang, R.; Yavuz, M. S.; Yumak, H.; Ozturk, B.; Sheng, J.; Yigit, M. V., Discriminating a Single Nucleotide Difference for Enhanced miRNA Detection Using Tunable Graphene and Oligonucleotide Nanodevices. *Langmuir* **2015**, 31, 9943-9952.